

# Analysis of the thermoelectric properties of *n*-type ZnO

Khuong P. Ong,<sup>1</sup> David J. Singh,<sup>2</sup> and Ping Wu<sup>1</sup>

<sup>1</sup>*Institute of High Performance Computing, 1 Fusionopolis Way, Singapore 138632*

<sup>2</sup>*Materials Science and Technology Division, Oak Ridge National Laboratory, Oak Ridge, Tennessee 37831-6114, USA*

(Received 8 December 2010; revised manuscript received 1 February 2011; published 7 March 2011)

We report an investigation of the temperature- and doping-dependent thermoelectric behavior of *n*-type ZnO. The results are based on a combination of experimental data from the literature and calculated transport functions obtained from Boltzmann transport theory applied to the first-principles electronic structure. From this we obtain the dependence of the figure of merit  $ZT$  on doping and temperature. We find that improvement of the lattice thermal conductivity is essential for obtaining high  $ZT$  in *n*-type ZnO.

DOI: [10.1103/PhysRevB.83.115110](https://doi.org/10.1103/PhysRevB.83.115110)

PACS number(s): 72.20.My, 72.15.Eb

## I. INTRODUCTION

There is current interest in high-temperature thermoelectric materials both for space applications such as radioisotope thermoelectric generators and more recently for solar-thermal electrical-energy production. In both applications the efficiency depends on the operating temperature, with higher temperature yielding higher efficiency, and also on the thermoelectric performance of the materials, which is characterized by a dimensionless figure of merit  $ZT = \sigma S^2 T / \kappa$ , where  $\sigma$  is the electrical conductivity,  $S$  is the thermopower,  $T$  is temperature, and  $\kappa$  is the thermal conductivity, normally the sum of electronic and lattice contributions,  $\kappa = \kappa_e + \kappa_l$ . The transport functions determining  $ZT$ , and therefore  $ZT$  itself, are temperature dependent. Actual device performances are determined by averages over the operating temperature range. In any case, because of the very high temperatures that can be achieved with concentrated sunlight, the development of low-cost environmentally friendly thermoelectric materials that can operate at very high temperatures may be of considerable value in solar-thermal applications.

ZnO is of particular interest in this regard. This compound is a potentially low-cost, nontoxic *n*-type semiconductor that is stable in air up to very high temperatures in excess of 1300 °C, especially when alloyed with electropositive trivalent elements such as Al.<sup>1</sup> The decomposition temperature of ZnO is above 2200 K. There is a large body of experimental data available especially on ambient-temperature properties of semiconducting ZnO.<sup>2,3</sup> Also, there has been substantial recent interest in doped ZnO as an oxide thermoelectric.<sup>1,4–16</sup> Here we use a combination of first-principles calculations and analysis of existing experimental data to investigate the potential of *n*-type ZnO as a very high temperature thermoelectric.

## II. APPROACH

Our approach is along the lines that were used previously for PbSe.<sup>17</sup> Specifically, we use Boltzmann transport theory based on the first-principles electronic structure to obtain the temperature and doping-level ( $n$ ) dependencies of the thermopower,  $S(T, n)$ , and the ratio  $\sigma/\tau$ , where  $\tau^{-1}$  is the electronic-scattering rate. We then combine this with models fixed by existing experimental data for the  $T$  and  $n$  dependencies of  $\tau$  and the  $T$  dependence of the lattice part of

the thermal conductivity,  $\kappa_l$ . We use this combination to obtain the  $T$  and  $n$  dependencies of the transport quantities, including  $ZT$ .

We used the electronic structure as obtained with the general potential linearized augmented plane wave (LAPW) method including local orbitals,<sup>18,19</sup> as implemented in the WIEN2k code.<sup>20</sup> We used LAPW sphere radii of 2.05 bohrs for Zn and 1.60 bohrs for O. Core states were treated relativistically, while we used the scalar relativistic treatment for the valence states. We used well-converged basis sets and Brillouin-zone samplings, and particularly tested the convergence of the transport properties at different dopings and temperatures with respect to zone sampling. We used the experimental wurtzite crystal structure ( $a = 3.2489$  Å,  $c = 5.2049$  Å,  $z_O = 0.381$ ), with the recently developed exchange-correlation functional of Tran and Blaha, which we denote here as TB-mBJ.<sup>21</sup> This functional substantially improves the band gaps of simple semiconductors and insulators with respect to standard local-density and generalized-gradient approximation methods, and in particular improves the band structure of ZnO.<sup>21–23</sup>

The calculated band structure is shown in Fig. 1. While our band gap of 2.65 eV remains smaller than the experimental gap of 3.4 eV, it is large enough to prevent bipolar transport for the doping levels and temperatures that we consider here; i.e., it is enough to avoid artifacts that arise from exaggerated minority carrier contributions to transport that would result from a too small gap. For comparison, the gap obtained in the same way but with the standard generalized-gradient approximation of Perdew, Burke, and Ernzerhof<sup>24</sup> is 0.8 eV, while the local-density approximation gap is 0.7 eV. The calculated gap with the Engel-Vosko GGA,<sup>25</sup> which is sometimes used to improve semiconductor band gaps, is 1.3 eV.

As has been emphasized in the past,<sup>3</sup> the electronic structure shows a very strong asymmetry between electrons and holes. Here we focus on *n*-type materials, but we note that the thermoelectric properties of *p*-type would be very different, and in fact the multiple heavy bands near the valence-band maximum suggest that the *p*-type would perhaps be a better thermoelectric material if it were possible to make it.

The temperature and doping level dependent thermopower and other transport functions were obtained from the electronic structure using the standard Boltzmann transport theory<sup>26</sup> within the constant scattering time approximation (CSTA). This approach has been shown to provide a good description

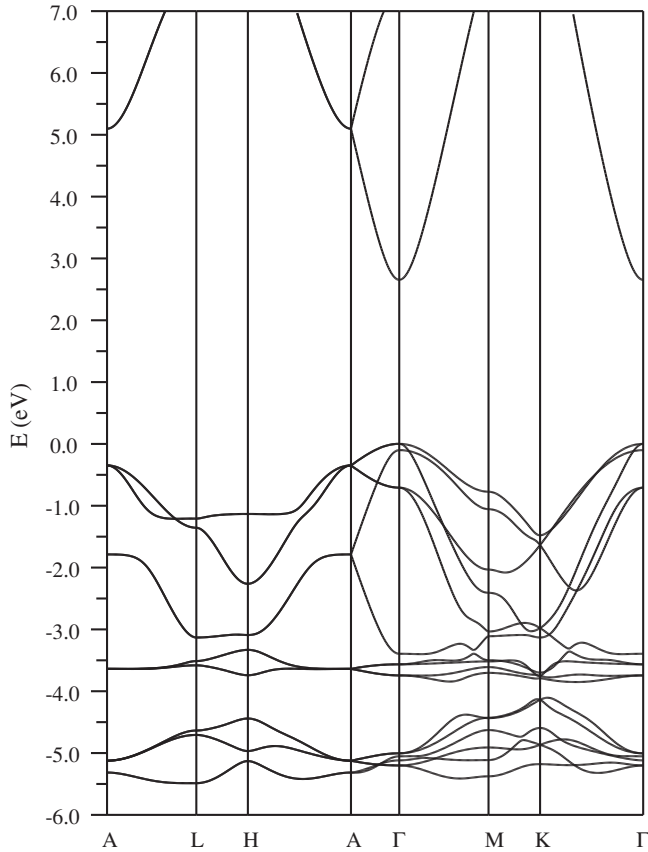


FIG. 1. Calculated band structure of ZnO using the TB-mBJ functional. The energy zero is at the valence-band maximum. Note the light, isotropic conduction band and the much heavier, anisotropic valence bands.

of  $S(T)$  in a variety of thermoelectric materials, including conventional thermoelectrics and oxides.<sup>27-33</sup> The main approximation is the assumption that the energy dependence of the scattering rate is weak compared to the energy dependence of the electronic structure, i.e., the CSTA. No assumption is made about the temperature or doping-level dependence of the scattering. The detailed formulas used are given in Ref. 34. These were evaluated using the BoltzTraP code.<sup>35</sup>

### III. THERMOPOWER

The thermopower plays a central role in thermoelectric performance. With use of the Wiedemann-Franz relation for the electronic part of the thermal conductivity,  $\kappa_e = L\sigma T$ , the figure of merit can be expressed as  $ZT = rS^2/L$ , where  $r = \kappa_e/\kappa_l \leq 1$ , emphasizing the fact that high  $ZT$  cannot be obtained without high  $S$ . This expression also makes clear that low lattice thermal conductivity is important since  $r$  will be low if  $\kappa_l$  is large compared to  $\kappa_e$ .

The thermopower is directly fixed by the electronic structure with no adjustable parameters within the CSTA. This is because the scattering rate cancels in the formula for  $S(T, n)$ . The calculated result is shown in Fig. 2 for the  $a$ -axis and  $c$ -axis directions. There is very little anisotropy, which is also the case for the other  $n$ -type transport functions. This is not the case for  $p$ -type (not shown). In the following, we

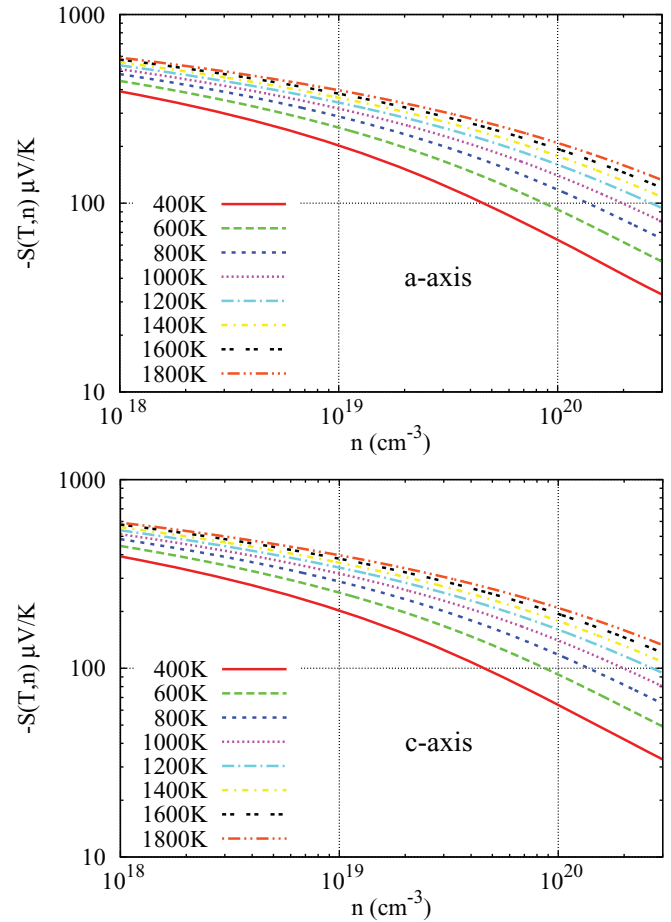


FIG. 2. (Color online) Calculated  $S(T, n)$  for ZnO in the  $a$ -axis (top) and  $c$ -axis (bottom) directions.

only show the  $a$ -axis direction transport quantities. According to our calculations the  $c$ -axis transport is slightly more favorable.

Importantly, because of the substantial band gap, there is no bipolar conduction, and so the thermopower continues increasing with  $T$  to the highest temperatures, even at low doping. Furthermore, high thermopowers are obtained at reasonable doping levels when one goes to high temperature. This result is in accord with existing experimental data, which do show high thermopowers at high  $T$  in heavily doped samples,<sup>1,9,16</sup> although we cannot compare directly because the precise carrier concentrations in the experimental samples are not known. For example, according to our calculations, at 1000 °C thermopowers in excess of 160  $\mu\text{V/K}$  are obtained up to  $n = 10^{20} \text{ cm}^{-3}$ . If the lattice thermal conductivity were negligible at this temperature ( $r = 1$ ), this value of  $S$  would correspond to  $ZT = 1$ .

### IV. ELECTRICAL CONDUCTIVITY

Using the electronic structure it is possible to calculate  $\sigma/\tau$  as a function of  $n$  and  $T$ , but it is not possible to calculate  $\sigma$  itself without knowledge of the scattering rate  $\tau^{-1}$ . In order to proceed, we use experimental data, which ideally should come from thermoelectric samples, since in that case the extrapolation will be over a smaller range. For this

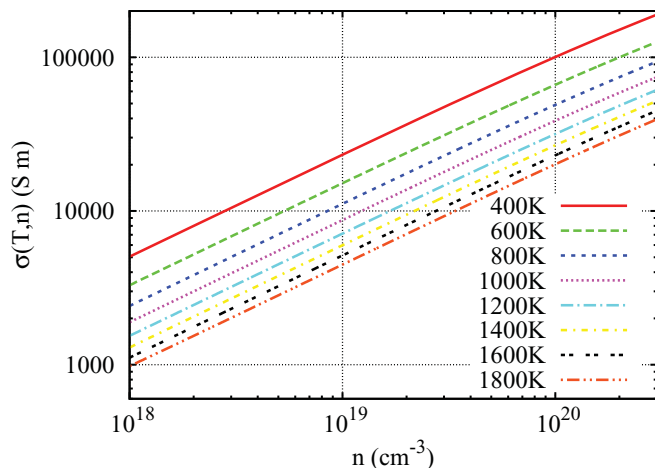


FIG. 3. (Color online) Calculated conductivity of ZnO as a function of  $T$  and  $n$  (see text).

purpose, we used 900 °C data from Ohtaki and coworkers,<sup>1</sup> who made measurements on ceramic material. They report a thermopower  $S = -200 \mu\text{V/K}$  at this temperature. By comparing with the calculated  $S(T, n)$  (Fig. 2), we obtain a value  $n = 5.4 \times 10^{19} \text{ cm}^{-3}$  for this sample. The reported experimental resistivity is  $4.5 \times 10^{-5} \Omega\text{m}$ , which combined with the calculated  $\sigma/\tau$  yields  $\tau = 5.7 \times 10^{-15} \text{ s}$  for this particular sample at 900 °C. In this regime, the experimental data from this sample and others follow an approximate electron-phonon  $T$  dependence  $\sigma \propto T^{-1}$ . For the doping dependence, we therefore take a standard electron-phonon form,  $\tau \propto n^{-1/3}$ . This yields  $\tau = 2.53 \times 10^{-5} T^{-1} n^{-1/3}$  with  $\tau$  in s,  $T$  in K, and  $n$  in  $\text{cm}^{-3}$ . As mentioned, we then calculate  $\sigma$  as  $\sigma/\tau \times \tau$ . The resulting  $a$ -axis conductivity is shown in Fig. 3. The high- $T$   $c$ -axis conductivity is somewhat higher (by 2%–3% depending on  $T$  and  $n$ ), but not significantly so.

The corresponding power factor  $\sigma S^2$ , obtained from the calculated  $S(T, n)$  and  $\sigma$  as above, is given in Fig. 4. The peak power factor is only very weakly  $T$  dependent with a value  $(\sigma S^2)_{\text{max}} \sim 0.001 \text{ W/mK}^2$ . However, the peak shifts to higher doping levels with  $T$ , e.g., from  $n = 6 \times 10^{18} \text{ cm}^{-3}$  at 400 K to  $n = 4 \times 10^{19} \text{ cm}^{-3}$  at

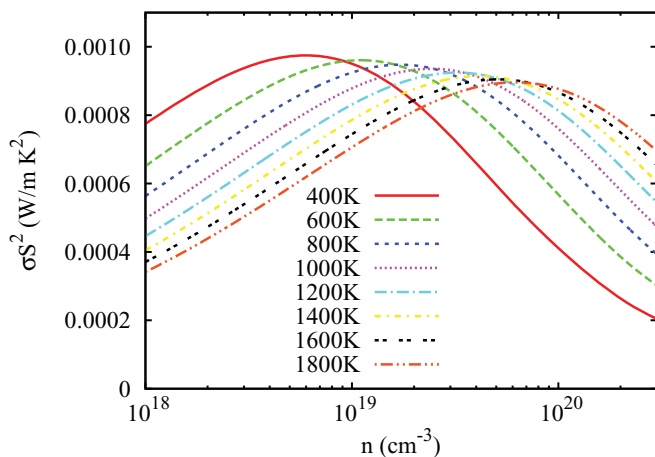


FIG. 4. (Color online) Calculated power factor  $\sigma S^2$  based on the data in Figs. 2 and 3.

1200 K. As has been emphasized previously,<sup>1,4,13,16</sup> power factors in this range make ZnO comparable to other known good thermoelectric materials. Importantly, for the doping level corresponding to the peak power factor, the thermopower is also high. At 1200 K and  $n = 4 \times 10^{19} \text{ cm}^{-3}$  the calculated thermopower is  $225 \mu\text{V/K}$ .

## V. THERMAL CONDUCTIVITY

The thermal conductivity consists of a sum of electronic and lattice contributions. For the electronic part we use the Wiedemann-Franz relation,  $\kappa_e = L\sigma T$ , with the standard value,  $L = 2.45 \times 10^{-8} \text{ W}\Omega/\text{K}^2$ . As mentioned, the electronic thermal conductivity sets the scale for the requirement of low lattice thermal conductivity for high  $ZT$  through the factor  $r = \kappa_e/(\kappa_e + \kappa_l)$ .

The thermal conductivity of single-crystal ZnO was investigated from 4.2 K to 300 K by Slack.<sup>36</sup>  $\kappa$  is weakly anisotropic and has a maximum at  $\sim 30$  K, approaching the expected Umklapp phonon scattering  $1/T$  behavior between 150 and 300 K. The single-crystal value at 300 K of  $\kappa = 54 \text{ W m}^{-1} \text{ K}^{-1}$  is very high for a thermoelectric material. However, it should be emphasized that ZnO is clearly not a good thermoelectric material at ambient  $T$ , but rather is investigated for possible high  $ZT$  at high  $T$ . Therefore we consider the high-temperature properties of ceramic thermoelectric samples.

There have been a number of studies of the thermal conductivity of dense ceramic ZnO at elevated  $T$ .<sup>1,3–5,9,10,16,37,38</sup> As a starting point, we may take the ambient-temperature value of  $37.5 \text{ W m}^{-1} \text{ K}^{-1}$  from Ref. 37, which is also consistent with the data reported by Ohtaki and coworkers,<sup>1</sup> for the sample that we used to fix the scattering rate. At this temperature the electronic contribution to the thermal conductivity is negligible, and so we have  $\kappa_l(300 \text{ K}) = 37.5 \text{ W m}^{-1} \text{ K}^{-1}$ . One might then assume a  $1/T$  temperature dependence of  $\kappa_l$  and proceed to estimate  $ZT$  using this and the electrical properties discussed above. However, these data, which were obtained from dense ceramic based on sintered nanosize powder, shows large deviations from  $1/T$ . In particular, the thermal conductivity at high  $T$  is much lower than would be obtained from this extrapolation. Furthermore, all the ceramic ZnO data mentioned above show the same feature,<sup>1,4,5,9,10,16,37,38</sup> including old dense-ceramic data from the 1950s.<sup>38</sup> That is, all the reported high- $T$  thermal-conductivity data fall below the  $1/T$  extrapolation from ambient temperature, although the details vary, perhaps because of sample dependence.

Such a decrease in thermal conductivity can be due to a softening of the lattice at high temperatures, i.e., a reduction in lattice stiffness leading to reduced sound velocities, or since all the samples are very fine ceramics, it could be an effect of nanostructuring. One interesting possibility is that anisotropic thermal expansion could lead to increased phonon scattering in fine-grained ceramics due to inhomogeneous stress fields. In fact, the thermal expansion of ZnO at high  $T$  is large and substantially anisotropic, with  $a$ - and  $c$ -axis values of  $\alpha_a = 8 \times 10^{-6}$  and  $\alpha_c = 5 \times 10^{-6}$ , respectively.<sup>39</sup> It will be of interest to measure the high-temperature thermal conductivity of single-crystal ZnO to sort out the actual mechanism by which  $\kappa_l$  decreases faster than  $1/T$ .

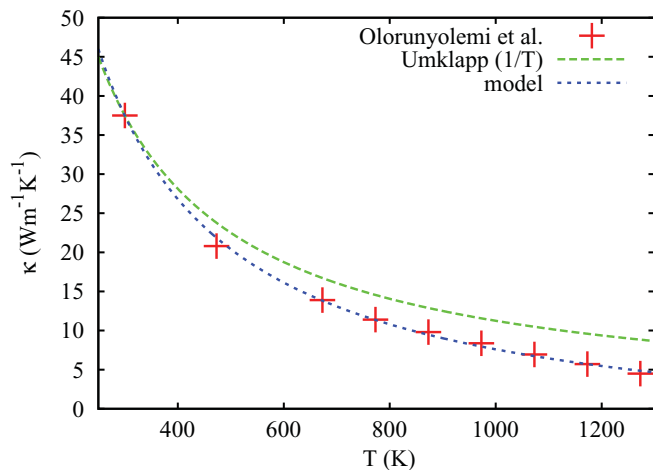


FIG. 5. (Color online) Thermal conductivity of ZnO from Ref. 37 compared with an Umklapp  $1/T$  form matched to the ambient-temperature value and the fit to experimental data used on our model as discussed in the text.

We used the data of Olorunyolemi and coworkers<sup>37</sup> to model  $\kappa_l$ . This choice was made because the data are for nominally undoped material and so we do not need to correct for an electronic contribution, which in turn would depend on knowledge of the conductivity, and also because, as mentioned, the thermal conductivity is consistent with the data reported by Ohtaki and coworkers for the sample that we used to fix the scattering rate for the electrical properties. A very good description of the experimental data can be obtained using the functional form  $\kappa = (A - BT)/T$ , with  $A = 12800 \text{ W m}^{-1}$  and  $B = 5.2 \text{ W m}^{-1} \text{ K}^{-1}$ . This is shown in Fig. 5.

In any case, this fit completes the model for transport, so that we can calculate  $ZT$  as a function of  $T$  and  $n$ . This is shown in Fig. 6. We note that the model has a number of assumptions, particularly regarding the experimental data that are taken as representing the intrinsic behavior of ZnO. However, we can use it to obtain semiquantitative information

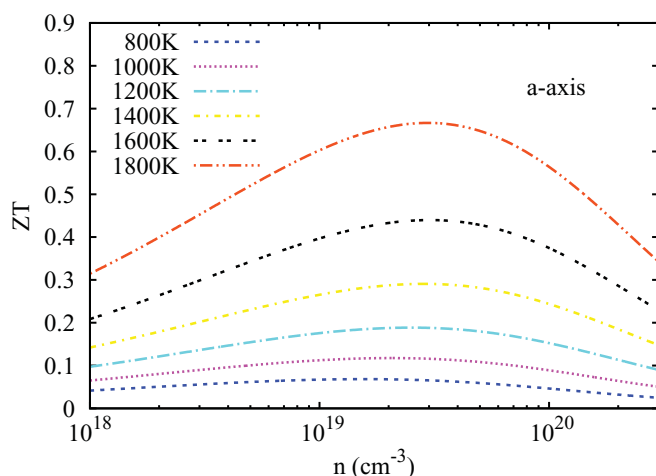


FIG. 6. (Color online) Calculated  $ZT(T, n)$  of  $n$ -type ZnO using the model discussed in the text. The data shown are for the  $a$ -axis direction. The  $c$ -axis data are very similar although the peak  $ZT$  is slightly higher for  $c$ .

about the behavior of  $ZT$  with doping and temperature. As may be seen,  $ZT$  is a strongly increasing function of  $T$  up to the highest  $T$ . This is because of two effects. First of all, the thermopower increases with  $T$  due to the large band gap. Second, because the electronic thermal conductivity has only weak  $T$  dependence while the lattice thermal conductivity strongly decreases, there is a strong increase in the factor  $r$  with  $T$ . The optimum doping level at high  $T$  is in the range from  $2 \times 10^{19} \text{ cm}^{-3}$  to  $6 \times 10^{19} \text{ cm}^{-3}$ . The calculated peak values of  $ZT$  are comparable to the best experimental samples reported at a given  $T$ . Thus the calculations suggest that reported high- $ZT$  samples in the literature are essentially fully optimized with respect to doping so that large further increases in  $ZT$  from tuning the carrier concentration are unlikely.

## VI. DISCUSSION AND CONCLUSIONS

The key question is then whether it is possible to obtain high  $ZT$  of unity or above in  $n$ -type ZnO at practical temperatures. Based on the results above, the best experimental samples are well optimized and therefore it would seem that this is unlikely through fine tuning of the carrier concentration in standard ZnO. Since the mobility at high  $T$  is fixed by electron-phonon scattering, it seems likely that improvements in the electrical conductivity will be limited. However, the ratio  $r = \kappa_e/\kappa$  mentioned above provides some insight into the reason why  $ZT$  is not higher.

We plot the calculated  $r$  from our model in Fig. 7. As may be seen,  $r$  is substantially lower than unity for the doping levels where the peak  $ZT$  is found. This means that although the power factor and thermopower are both quite reasonable, the lattice thermal conductivity is strongly constraining  $ZT$ , and therefore that much better values of  $ZT$  would result if  $\kappa_l$  could be reduced. In fact, according to our model, if the lattice thermal conductivity is arbitrarily reduced to  $1/3$  of its value, keeping the other parameters fixed, we obtain  $ZT = 1$  at 1600 K, with a doping level of  $\sim 2 \times 10^{19} \text{ cm}^{-3}$ . While at first sight this may seem unrealistic, we note that the thermal conductivity in fine-grained dense ceramic does fall faster than  $1/T$ . If this is in fact a result of nanoscale stress inhomogeneities, it may well be that further reductions

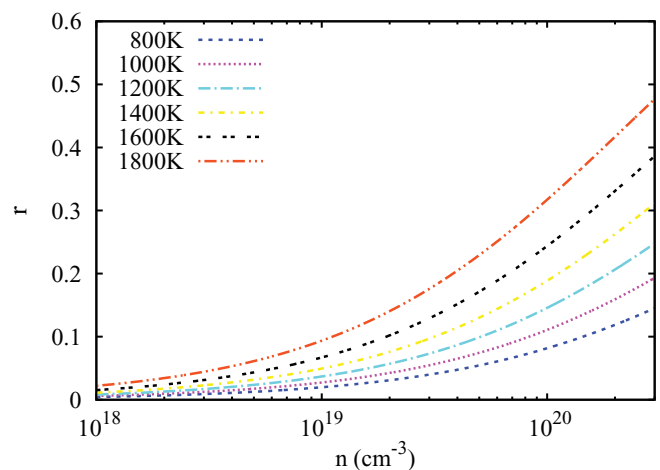


FIG. 7. (Color online) Calculated  $r = \kappa_e/\kappa$  for the model discussed in the text. The data shown are for the  $a$ -axis direction.

are possible through control of the grain size and ceramic texture. Also, it may be possible to introduce nanostructure into thermoelectric ZnO by other means than sintering of nanosize powders. In particular, it may be possible to use nanoprecipitates or spinodal decomposition, as for example in ZnO with Co and Ni<sup>40,41</sup> and possibly in ZnO co-doped with Mn and Al.<sup>42</sup> In fact, it has been reported that co-addition of Al<sub>2</sub>O<sub>3</sub> and NiO improves the thermoelectric properties of *n*-type ZnO.<sup>9</sup>

In any case, it will be of considerable interest to study the high-temperature thermal conductivity of ZnO single crystals and ceramics produced with different grain sizes and textures to better understand the origin of the reduced high-*T* lattice thermal conductivity and whether it is possible to obtain

further reductions. Similarly, it will be desirable to investigate in more detail the use of nanostructuring to modify thermal conductivity in ZnO.

#### ACKNOWLEDGMENTS

This work was supported by the US Department of Energy, Basic Energy Sciences, through the S3TEC Energy Frontier Research Center (D.J.S.), the Institute of High Performance Computing (IHPC) (K.P.O. and P.W.), and the Agency of Science, Technology, and Research (A\*STAR) (K.P.O. and P.W.). D.J.S. is very grateful for the hospitality of the IHPC where a portion of this work was performed.

- 
- <sup>1</sup>M. Ohtaki, T. Tsubota, K. Eguchi, and H. Arai, *J. Appl. Phys.* **79**, 1816 (1996).
- <sup>2</sup>S. J. Pearton, D. P. Norton, K. Ip, Y. W. Heo, and T. Steiner, *Prog. Mater. Sci.* **50**, 293 (2005).
- <sup>3</sup>U. Ozgur, Y. I. Alivov, C. Liu, A. Teke, M. A. Reshchikov, S. Dogan, V. Avrutin, S. J. Cho, and H. Morkoc, *J. Appl. Phys.* **98**, 041301 (2005).
- <sup>4</sup>T. Tsubota, M. Ohtaki, K. Eguchi, and H. Arai, *J. Mater. Chem.* **7**, 85 (1997).
- <sup>5</sup>T. Tsubota, M. Ohtaki, K. Eguchi, and H. Arai, *J. Mater. Chem.* **8**, 409 (1998).
- <sup>6</sup>M. Ueno, Y. Yoshida, Y. Takai, and M. Yamaguchi, *J. Ceram. Soc. Jpn.* **112**, 327 (2004).
- <sup>7</sup>S. Katsuyama, Y. Takagi, M. Ito, K. Majima, N. Nagai, H. Sakai, K. Yoshimura, and K. Kosuge, *J. Appl. Phys.* **92**, 1391 (2002).
- <sup>8</sup>Y. Fujishiro, M. Miyata, M. Awano, and K. Maeda, *J. Am. Ceram. Soc.* **87**, 1890 (2004).
- <sup>9</sup>K. H. Kim, S. H. Shim, K. B. Shim, K. Nihara, and J. Hojo, *J. Am. Ceram. Soc.* **88**, 628 (2005).
- <sup>10</sup>H. Kaga, Y. Kinemuchi, S. Tanaka, A. Mayika, Z. Kato, K. Uematsu, and K. Watari, *Jpn. J. Appl. Phys.* **45**, L1212 (2006).
- <sup>11</sup>S. Isobe, T. Tani, Y. Masuda, W. S. Seo, and K. Kuomoto, *Jpn. J. Appl. Phys.* **41**, 731 (2002).
- <sup>12</sup>B. A. Cook, J. L. Harringa, and C. B. Vining, *J. Appl. Phys.* **83**, 5858 (1998).
- <sup>13</sup>Y. Kinemuchi, C. Ito, H. Kaga, T. Aoki, and K. Watari, *J. Mater. Res.* **22**, 1942 (2007).
- <sup>14</sup>J. P. Wiff, Y. Kinemuchi, and K. Watari, *Mater. Lett.* **63**, 2470 (2009).
- <sup>15</sup>J. P. Wiff, Y. Kinemuchi, H. Kaga, C. Ito, and K. Watari, *J. Eur. Ceram. Soc.* **29**, 1413 (2009).
- <sup>16</sup>M. Ohtaki, K. Araki, and K. Yamamoto, *J. Electron. Mater.* **38**, 1234 (2009).
- <sup>17</sup>D. Parker and D. J. Singh, *Phys. Rev. B* **82**, 035204 (2010).
- <sup>18</sup>D. J. Singh and L. Nordstrom, *Planewaves, Pseudopotentials, and the LAPW Method*, 2nd ed. (Springer, Berlin, 2006).
- <sup>19</sup>E. Sjoestedt, L. Nordstrom, and D. J. Singh, *Solid State Commun.* **114**, 15 (2000).
- <sup>20</sup>P. Blaha, K. Schwarz, G. Madsen, D. Kvasnicka, and J. Luitz, WIEN2k, An Augmented Plane Wave + Local Orbitals Program for Calculating Crystal Properties, Tech. Univ. Wien, Austria, 2001.
- <sup>21</sup>F. Tran and P. Blaha, *Phys. Rev. Lett.* **102**, 226401 (2009).
- <sup>22</sup>D. J. Singh, *Phys. Rev. B* **82**, 155145 (2010).
- <sup>23</sup>D. J. Singh, *Phys. Rev. B* **82**, 205102 (2010).
- <sup>24</sup>J. P. Perdew, K. Burke, and M. Ernzerhof, *Phys. Rev. Lett.* **77**, 3865 (1996).
- <sup>25</sup>E. Engel and S. H. Vosko, *Phys. Rev. B* **47**, 13164 (1993).
- <sup>26</sup>J. M. Ziman, *Electrons and Phonons* (Oxford University Press, New York, 2001).
- <sup>27</sup>D. J. Singh and I. I. Mazin, *Phys. Rev. B* **56**, R1650 (1997).
- <sup>28</sup>G. K. H. Madsen, K. Schwarz, P. Blaha, and D. J. Singh, *Phys. Rev. B* **68**, 125212 (2003).
- <sup>29</sup>H. J. Xiang and D. J. Singh, *Phys. Rev. B* **76**, 195111 (2007).
- <sup>30</sup>A. F. May, D. J. Singh, and G. J. Snyder, *Phys. Rev. B* **79**, 153101 (2009).
- <sup>31</sup>L. L. Wang, L. Miao, Z. Y. Wang, W. Wei, R. Xiong, H. J. Liu, J. Shi, and X. F. Tang, *J. Appl. Phys.* **105**, 013709 (2009).
- <sup>32</sup>S. G. Kim, I. I. Mazin, and D. J. Singh, *Phys. Rev. B* **57**, 6199 (1998).
- <sup>33</sup>D. J. Singh, *Phys. Rev. B* **81**, 195217 (2010).
- <sup>34</sup>L. Zhang and D. J. Singh, *Phys. Rev. B* **80**, 075117 (2009).
- <sup>35</sup>G. K. H. Madsen and D. J. Singh, *Comput. Phys. Commun.* **175**, 67 (2006).
- <sup>36</sup>G. A. Slack, *Phys. Rev. B* **6**, 3791 (1972).
- <sup>37</sup>T. Olorunyolemi, A. Birnboim, Y. Carmel, O. C. Wilson Jr., and I. K. Lloyd, *J. Am. Ceram. Soc.* **85**, 1249 (2002).
- <sup>38</sup>W. D. Kingery, J. Francl, R. L. Coble, and T. Vasilos, *J. Am. Ceram. Soc.* **37**, 107 (1954).
- <sup>39</sup>H. Ibach, *Phys. Status Solidi* **33**, 257 (1969).
- <sup>40</sup>M. A. White, S. T. Ochsenein, and D. R. Gamelin, *Chem. Mater.* **20**, 7107 (2008).
- <sup>41</sup>S. Zhou, K. Potzger, J. von Borany, R. Grotzschel, W. Skorupa, M. Helm, and J. Fassbender, *Phys. Rev. B* **77**, 035209 (2008).
- <sup>42</sup>X. Li, Z. Yu, X. Long, P. Lin, X. Cheng, Y. Liu, C. Cao, H. Zhang, G. Wu, and R. Yu, *Appl. Phys. Lett.* **94**, 252501 (2009).